PHOTOGRAPH THIS SHEET

DTIC FILE COPY

LEVEL

INVENTORY 1

AD-A202 550

DTIC ACCESSION NUMBER

ETL-0448

DOCUMENT IDENTIFICATION

Dec 1986

This document has been approved for public release and sale; its distribution is unlimited.

DISTRIBUTION STATEMENT

ACCESSION FOR	
NTIS	GRA&I ☒
DTIC	TAB ☐
UNANNOUNCED	☐
JUSTIFICATION	
BY	
DISTRIBUTION /	
AVAILABILITY CODES	
DIST	AVAIL AND/OR SPECIAL
A-1	END 23

DISTRIBUTION STAMP

DTIC COPY INSPECTED 6

DTIC ELECTE DEC 01 1988 S D E

DATE ACCESSIONED

DATE RETURNED

88 11 30 125

DATE RECEIVED IN DTIC

REGISTERED OR CERTIFIED NO.

PHOTOGRAPH THIS SHEET AND RETURN TO DTIC-FDAC

DTIC FORM 70A MAR 86

DOCUMENT PROCESSING SHEET

PREVIOUS EDITION MAY BE USED UNTIL STOCK IS EXHAUSTED.

ETL-0448

Local gravity field modeling

Eugene J. Rose

December 1986

Prepared for
U.S. ARMY CORP OF ENGINEERS
ENGINEER TOPOGRAPHIC LABORATORIES
FORT BELVOIR, VIRGINIA 22060-5546

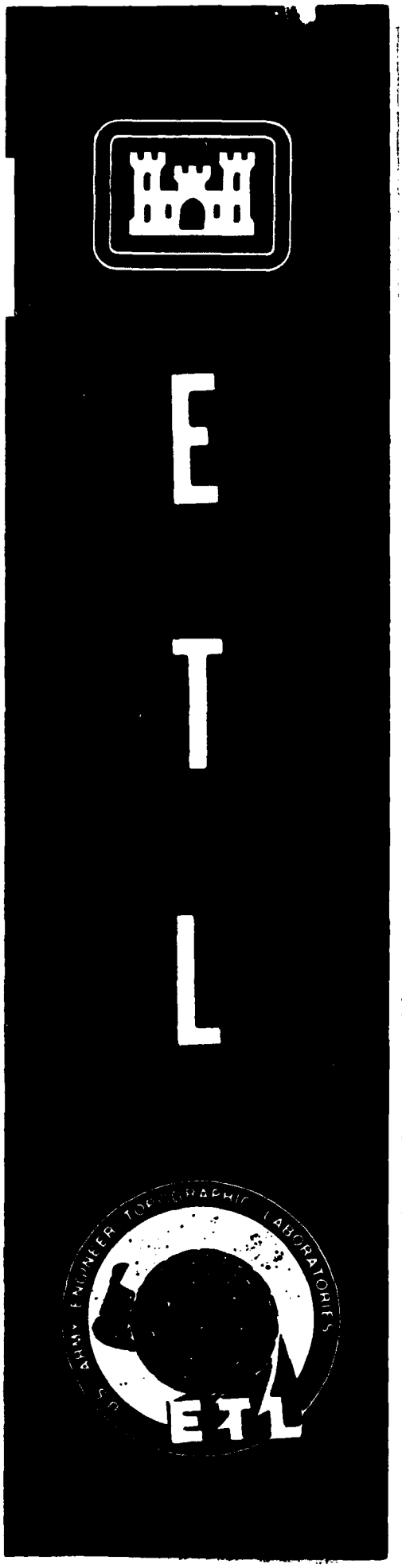

Destroy this report when no longer needed.
Do not return it to the originator.

The findings in this report are not to be construed as an official Department of the Army position unless so designated by other authorized documents.

The citation in this report of trade names of commercially available products does not constitute official endorsement or approval of the use of such products.

DISCLAIMER NOTICE

THIS DOCUMENT IS BEST QUALITY PRACTICABLE. THE COPY FURNISHED TO DTIC CONTAINED A SIGNIFICANT NUMBER OF PAGES WHICH DO NOT REPRODUCE LEGIBLY.

UNCLASSIFIED

SECURITY CLASSIFICATION OF THIS PAGE *(When Data Entered)*

REPORT DOCUMENTATION PAGE		READ INSTRUCTIONS BEFORE COMPLETING FORM
1. REPORT NUMBER ETL-0448	2. GOVT ACCESSION NO.	3. RECIPIENT'S CATALOG NUMBER
4. TITLE *(and Subtitle)* LOCAL GRAVITY FIELD MODELING		5. TYPE OF REPORT & PERIOD COVERED Technical Report 6. PERFORMING ORG. REPORT NUMBER
7. AUTHOR(s) U.S. Army Engineer Topographic Laboratories Fort Belvoir, Virginia 22060-5546		8. CONTRACT OR GRANT NUMBER(s)
9. PERFORMING ORGANIZATION NAME AND ADDRESS U.S. Army Engineer Topographic Laboratories Fort Belvoir, Virginia 22060-5546		10. PROGRAM ELEMENT, PROJECT, TASK AREA & WORK UNIT NUMBERS 4A762707A855, A, 0030
11. CONTROLLING OFFICE NAME AND ADDRESS		12. REPORT DATE December 1986 13. NUMBER OF PAGES 50
14. MONITORING AGENCY NAME & ADDRESS(if different from Controlling Office)		15. SECURITY CLASS. (of this report) Unclassified 15a. DECLASSIFICATION DOWNGRADING SCHEDULE

16. DISTRIBUTION STATEMENT *(of this Report)*

Approved for public release; distribution is unlimited.

17. DISTRIBUTION STATEMENT *(of the abstract entered in Block 20, if different from Report)*

18. SUPPLEMENTARY NOTES

19. KEY WORDS *(Continue on reverse side if necessary and identify by block number)*

Deflection of the Vertical
Digital Terrain Models
Collocation
Geoid
Geoid Undulation
Geodesy
Gravity
Isostacy
Spherical Harmonics

20. ABSTRACT *(Continue on reverse side if necessary and identify by block number)*

In this report, an experiment is described wherein a local gravity field model was computed in mountainous terrain using digital terrain data, spherical harmonic coefficients, and local observations. The accuracies of free air gravity anomalies, deflections of the vertical, and geoid undulations computed are discussed.

DD FORM 1 JAN 73 1473 EDITION OF 1 NOV 65 IS OBSOLETE

UNCLASSIFIED

SECURITY CLASSIFICATION OF THIS PAGE *(When Data Entered)*

PREFACE

The work covered by this technical report was conducted by the U.S. Army Engineer Topographic Laboratories (ETL), Fort Belvoir, Virginia. It is part of an effort carried out on geodetic parameter estimation under DA project 4A762707A855, Work Unit 00030, entitled "Geodetic Parameters for Selected Missiles".

The work was conducted by Mr. Eugene Rose under the supervision of Mr. Peter Carvarich, Chief, Precise Survey Branch, Survey Division, Topographic Developments Laboratory. A special acknowledgement is made to Mr. Arch Carlson of the Defense Mapping Agency, Hydrographic-Topographic Center (DMAHTC) for valuable discussions and for providing us with several computer programs and observation data.

COL Alan L. Laubscher, CE, was Commander and Director and Mr. Walter E. Boge was Technical Director of ETL during the report preparation.

TABLE OF CONTENTS

ILLUSTRATIONS

TABLES

LOCAL GRAVITY FIELD MODELING

INTRODUCTION

Regional or local gravity field models are important for many applications. Deflections of the vertical and gravity anomalies are required for alignment and correction of high accuracy inertial navigation systems. Deflections are required to reduce observed horizontal and vertical angles to the ellipsoid, for instance in applying the Laplace correction to azimuths. They can be used to convert between astronomic and geodetic coordinates. Geoid undulations are required to convert between elevations derived from satellite observations, for example GPS, and heights above sea level. Undulations provide a direct map of the geoid in the region. Thus the important quantities to be derived from a model are gravity anomaly, deflections of the vertical and geoid undulations. In addition, one would like to be able to use, as observations in computing the model, all available geodetic data including: astro-geodetic deflections of the vertical, satellite derived geoid undulations, observed gravity values and computed anomalies, geodetic and astronomic coordinates, and spherical harmonic geopotential coefficients.

Of all available techniques, only least squares collocation allows one to use any combination of non-homogeneous geodetic data and to compute any of the required quantities. In addition, least squares collocation gives an optimal (minimum variance) method of interpolating among the survey

data. As with any prediction method, the results of least squares collocation depend on the variation of the gravity field in the area of prediction and on the density and accuracy of the available observations. In regions of sharply varying topography, a major portion of the variation of the gravity field is due to this topography. Since prediction results are nearly linearly related to the "smoothness" of the field, significant improvements can be obtained from least squares collocation in these cases by first removing a portion of this effect. In the past, this has been accomplished using rather coarse elevation models composed of mean elevations or elevations scaled from topographic maps (Forsberg and Tscherning, 1981a), (Forsberg and Madsen, 1980), (Junkel, 1982). The data spacing of these models has been on the order of 20 to 30 arc seconds.

This report describes an experiment conducted to compute a local gravity field model using least squares collocation in conjunction with several digital terrain models of varying resolution and extent. The most accurate elevation data was obtained photogrammetrically. In addition, a global trend is first removed by computing the spherical harmonic expansion of the anomalous potential from a 180 degree and order coefficient set, modified by the WGS72 ellipsoidal potential.

BACKGROUND

The U.S. Army Engineer Topographic Laboratories (USAETL) has been involved with developing hardware and software to support the Defense Mapping Agency (DMA) and other agencies in densifying and extending local gravity networks for many years. Recently, this work has been directed primarily to developing inertial surveying technology for determining gravity anomalies and deflections of the vertical as well as positions (Todd, 1982).

This work unit was initiated with the objective of examining other technologies and computational methods for computing magnitude and direction of the gravity vector and geoid undulations at a large number of points in a local region in an efficient way and with sufficient accuracy for some or any of the applications discussed above. In particular, computational techniques for combining large amounts of heterogeneous data were reviewed.

The interpolation of geodetic quantites is not so much a problem in flat areas. The gravity fields in these areas are smooth enough to be interpolated adequately for most purposes by standard least-squares methods (Heiskanen & Moritz, 1967). The determination of local gravity field models, or the determination of the geoid in mountainous areas is still very much a problem however. The scarcity of gravity data and the great irregularity of the field in

these areas make traditional methods ineffective. For these regions, least squares collocation following trend removal by spherical harmonic expansions and/or digital terrain models is a powerful tool which has been exploited in the Nordic nations (Forsberg & Knudsen, 1980), (Forsberg & Tscherning, 1981a), (Forsberg & Tscherning, 1981b), as well as in Europe (Gurtner & Elmiger, 1983), (Sunkel, 1983), and in Canada (Lachapelle, 1975). In addition, DMA has conducted in-house efforts. A report on these efforts (Carlson, 1983) was obtained. This report served as the starting point for the present research.

A review of these efforts indicated several areas in which further research could be focused. These include:

1. Effect of resolution and extent of digital terrain data on the accuracy of the solution.

2. Improvements to be gained by using a very dense DTM in the immediate vicinity of the computation point.

3. Effect of using only the terrain and isostatic data for trend removal, neglecting the spherical harmonic component.

4. Efficient methods for processing the terrain data including Fast Fourier Transforms (FFT).

5. Methods for the inclusion of geophysical information into the process.

This report addresses partially items (1) through (3) above. Further research will be required to more fully answer these issues and to address items (4) and (5) and others.

The next section briefly describes the method and the principles behind it. This is followed by a description of the test area and data used and by an analysis of each step of the process. The results are then presented, followed by some conclussions and recommendations.

DESCRIPTION OF THE TECHNIQUES

A body at rest on the earth's surface is acted upon by the gravitational attraction of the earth and the centrifugal force caused by the earth's rotation. The effect of the combination of these two forces is called gravity. The potential of gravity W is then the sum of the gravitational potential V and the centrifugal potential Φ.

Thus:

$$W = V + \Phi \qquad (1)$$

where:

$$V = k \iiint_v \frac{\rho}{l} dv \qquad (2)$$

and:

$$\Phi = \frac{1}{2} \omega^2 (x^2 + y^2) \qquad (3)$$

where:

k = the gravitational constant,
v = the volume of the earth,
ρ = the density of the earth,
l = the distance between the attracting mass and the attracted mass,
ω = the earth's rotational velocity,
x,y = the cartesian coordinates of the point

under consideration, in an earth-centered coordinate frame.

The gravity potential can also be expressed as the sum of a "normal" component U, which is due to a homogeneous ellipsoid of revolution which is an equipotential surface of a "normal" gravity field and a "disturbing" potential T, which is due to mass anomalies within the actual earth.

Thus:

$$W(x,y,z) = T(x,y,z) + U(x,y,z) \qquad 4$$

In U is also included the centrifugal potential and the effects of all masses external to the earth. Exterior to the earth, V satisfies Laplace's equation:

$$\Delta V = 0 \qquad 5$$

where Δ indicates the Laplacian operator:

$$\frac{\partial^2}{\partial x^2} + \frac{\partial^2}{\partial y^2} + \frac{\partial^2}{\partial z^2}$$

Thus it is a harmonic function external to the earth. Inside the earth, it is not harmonic because there V satisfies Poisson's equation:

$$V = -4\pi k\rho \qquad 6$$

The normal potential U can be computed directly for a given reference ellipsoid. All that is required is the specification of the four quantities:

a, semimajor axis; f, flattening

γ_a, equatorial gravity; and ω, angular velocity.

For this study, the WGS72 reference ellipsoid was used, the parameters taken from (DMA, 1974).

There remains then the computation of T, the "disturbing" or "anomalous" potential. From T we can derive all of the important quantities from the equations: (Heiskanen & Moritz, 1967)

gravity anomaly; $$\Delta g = -\frac{\partial T}{\partial r} - \frac{2}{r} T \qquad (7)$$

east-west deflection component; $$\eta = -\frac{1}{r\gamma\cos\varphi}\frac{\partial T}{\partial \lambda} \qquad (8)$$

north-south deflection component; $$\xi = -\frac{1}{r\gamma}\frac{\partial T}{\partial \varphi} \qquad (9)$$

geoid undulation; $$N = \frac{T}{\gamma_a} \qquad (10)$$

The technique under investigation is to break T into three parts. The first is a "global earth model" component due to an expansion of the anomalous potential into a spherical harmonic series. The second component is the topographic-isostatic component, computed from a regional or local model of the most well known mass anomalies, the topographic masses and their isostatic compensation. A third component is computed from a set of observed gravity anomalies, deflections of the vertical and geoid undulations in the local area of interest. This final component is the one actually computed by least squares collocation. Thus the model for the anomalous potential is:

$$T = T_{EM} + T_{TI} + T_{C} \qquad 11$$

where:

T_{EM} = the earth local component,
T_{TI} = the topographic-isostatic component, and
T_{C} = the residual component, or deviation from the model.

In frequency domain terms, we may consider the "signal" T to be broken down into the long wavelength component due to the spherical harmonics, a medium and short wavelength component due to the topography and its compensation and a residual component due to the deviation of the actual gravity field from the model.

There is however a problem with this concept in that the spherical harmonic coefficients contain some short wavelength information as well. We should therefore remove the topographic—isostatic effect on these coefficients before combining them with the other components. (Forsberg & Tscherning ,1981a) however have shown this effect to be negligible for fixed area computations for coefficients up to degree and order 36. Moreover, the effect of the higher degree and order coefficients will be nearly constant throughout a local area and thus this effect should be compensated by collocation.

The next section discusses the area studied and the data employed. The computation of each subcomponent of T is then explained in detail and the results are presented.

TEST AREA AND DATA

The principal test area lies in the eastern part of Nevada and is located between approximate north latitudes 37.5 and 38.5 degrees and west longitudes 114.5 and 115 degrees. The area is shown in figure 1. As can be seen in this figure, the area is nearly bisected by the Dry Lake Valley and is fairly mountainous outside of this valley. Elevations range from about 1400 meters in the valley to 2000 meters in the mountains.

From within this area, a set of 1344 gravity observations, 23 observed astro-geodetic deflections of the vertical and 6 geoid undulations obtained at doppler observation sites were obtained from DMA. All of the data was referenced to WGS72. From the gravity observations, free-air gravity anomalies were obtained from the formula:

$$\Delta g = g + .3086H - \text{gamma} \qquad (12)$$

where:

g = observed gravity at the earth's surface
.3086 = free-air normal gravity gradient in mgal/meter
H = height of the station above the geoid
gamma = normal gravity at the corresponding point on the ellipsoid.

A subset of 1062 of the gravity anomalies which lie within the principal test area were selected for initial

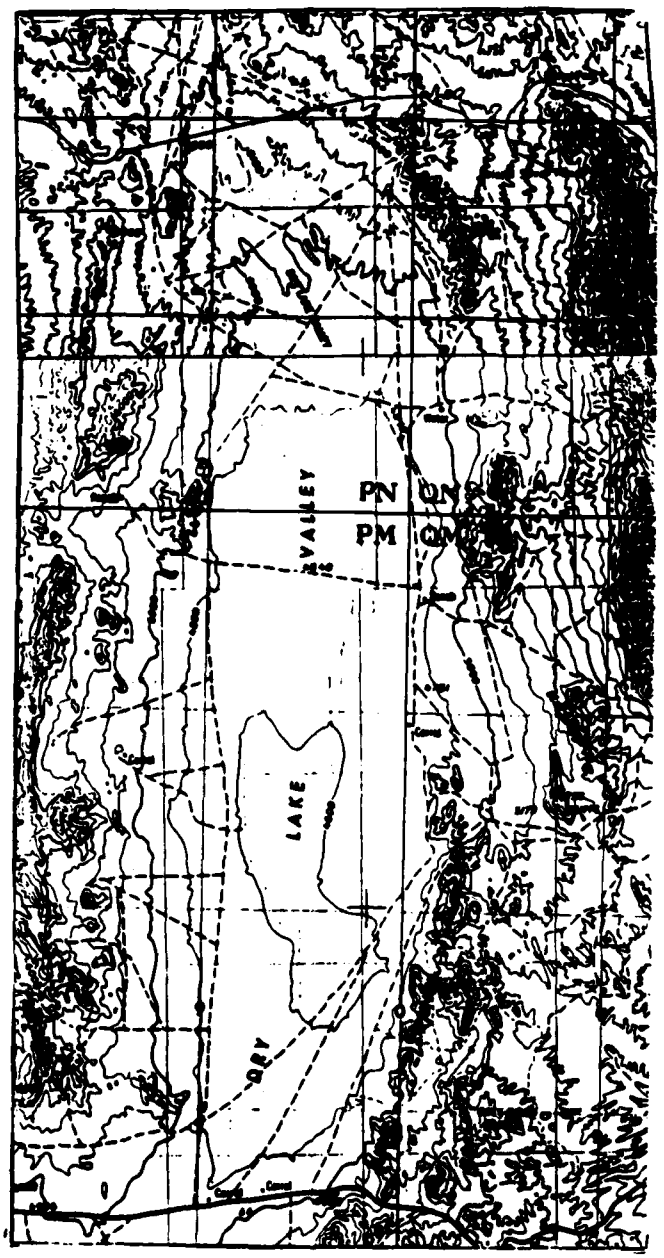

Figure 1. Test area.

analysis. The statistics of this data are given in table 1.

value	high	low	mean	s	n
Δg	63.0	-52.1	-13.5	22.70	1082
ksi	-1.44	-9.0	-4.3	1.80	23
eta	2.54	-12.4	-4.7	5.20	23
N	-24.69	-27.05	-25.50	1.05	6

Table 1. Statistics of observation data.

Digital elevation matrices covering the test area and surrounding areas were also obtained. The coarsest matrix has a spacing of 1 degree and dimensions of 10 degrees by 11 degrees, approximately centered on the principal test area. The next finer grid has spacing 5 minutes and has dimensions 5 by 6 degrees, again approximately centered on the test area. The final data set consisted of elevation values for the principal test area only. These elevations were derived from aerial photography of the test area. This data was not given on a grid but with irregular spacing. All of the elevation values are referenced to Mean Sea Level. The 1-degree and 5-minute data sets were derived from topographic maps and have an estimated horizontal accuracy of 100 to 300 meters and vertical accuracy of 20 to 150 meters. The vertical accuracy of the photogrammetric data is estimated to be under 10 feet, based on the flying height, camera, and stereoplotter used.

The photogrammetric data was supplied in approximate east-west profiles with a spacing between profiles of 500

feet. The spacing between points on the profiles is not constant but is less or equal to 500 feet. To compute the topographic and isostatic components of the gravity field, a program, described later, was used which requires the elevation values to be given on a square grid of latitude and longitude values. To obtain such a grid from the photogrammetric data, software was developed to interpolate elevation values at the nodes of the grid from surrounding values. If a data point was located within 50 feet of a node, the elevation of the node was taken to be that of the data point. Otherwise, a least squares fit of the surrounding elvations to the equation of a bilinear polynomial in x and y was performed.

To estimate the accuracy of this interpolated data set, the elevations supplied with the 1082 gravity observations were used. These were compared with weighted means of grid values from within a certain radius of the data points. Based on a comparison of 1066 well-spaced values, the RMS difference was plus-minus 43 feet.

The final data set used consisted of a 180 by 130 degree and order set of fully normalized spherical harmonic coefficients of the geopotential developed by (Rapp, 1981).

COMPUTATION OF THE MODEL

COMPUTATION OF THE GLOBAL EARTH MODEL COMPONENT

The equation for representing the earth's gravity potential W external to the attracting masses in terms of spherical harmonics is: (Heiskanen & Moritz, 1967)

$$W(r,\psi,\lambda) = \frac{kM}{r}\left[1 + \sum_{n=2}^{\infty}\left(\frac{a}{r}\right)^{n}\sum_{m=0}^{n}\left(\bar{C}_{nm}\cos(m\lambda) + \bar{S}_{nm}\sin(m\lambda)\right)\bar{P}_{nm}\sin(\psi)\right] + \Phi \quad (13)$$

where:

Φ = rotational potential,
r = geocentric distance,
ψ = geocentric latitude,
λ = longitude,
kM = the gravitational constant times the mass of the earth,

$\bar{C}_{nm}$, $\bar{S}_{nm}$ = the fully normalized spherical harmonic coefficients,

$\bar{P}_{nm}$ = the fully normalized associated Legendre polynomials,

a = the equatorial radius of the earth and,
n,m = the degree and order respectively.

In practice, of course, equation (13) cannot include an infinite number of terms. At the present time, the best solutions include terms up to degree and order 180. Examples are the Goddard Earth Model, GEM10C, and the solutions of Rapp (1978) and Rapp (1981). This last model was used in this study. To obtain T, the anomalous potential, we must subtract the potential of the reference ellipsoid. The

potential of the reference ellipsoid, U, may be written by setting all C and S in equation 13 equal to zero except the $C_{2,0}$ and $C_{4,0}$ terms.

Thus:

$$U(r,\psi,\lambda) = \frac{kM}{r}\left[1 + \left(\frac{a}{r}\right)^2 C^*_{2,0} P^*_{2,0} + \left(\frac{a}{r}\right)^4 C^*_{4,0} P_{4,0}\right] + \quad (14)$$

where:

$C^*_{2,0}$, $C^*_{4,0}$ = potential coefficients computed on the basis of the reference ellipsoid.

Subtracting equation (14) from equation (13) gives the desired T_{EM}. This calculation was carried out for all of the observation points using the spherical harmonic coefficients modified by subtracting the WGS72 ellipsoidal potential. The latitude of the points was first converted from geodetic to geocentric to conform to equations (13) and (14). The values of a, f, kM, $C_{2,0}$,and $C_{4,0}$ for the WGS ellipsoid were obtained from (DMA, 1974) The quantities of interest , Δg, ξ , η , and N , were obtained from equations 7 through 10.

For the purposes of this study, we are predicting gravimetric quantities at points where the values are known. Thus a direct measure of the accuracy of the computations is available. For the case of T_{EM} computed from spherical

harmonics, the results are summarized in table 2.

value	RMS error	mean error	std. dev. of error	n
Δg (mgal)	24.03	-6.40	23.16	1082
ksi (sec)	1.64	-0.26	1.62	23
eta (sec)	7.53	-3.24	6.76	23
N (m)	1.27	0.90	0.91	6

Table 2. Results of sperical harmonic computation.

Given the small number of undulations, conclusions are nearly impossible for these, however the solution does closely model the values available . The gravity anomaly vector is not well modeled by the solution however. One possible explanation is that the undulations are relatively unaffected by the short wavelength topography, which is not modeled by the solution while the gravity vector is highly dependant on the local topography and its isostatic compensation.

COMPUTATION OF THE TOPOGRAPHIC/ISOSTATIC COMPONENT OF T

The best known and most easily observable mass anomalies are those associated with the visible topography of the earth. Associated with the topography is the "isostatic compensation", or tendency of the topographic masses to be compensated by mass deficiencies within the earth's crust. The evidence of such compensation is given by the behavior of deflections and anomalies, especially Bouger

anomalies in mountainous areas. The Bouger reduction removes the main irregularities in the gravity field associated with the visible topography. Thus the values of Bouger anomalies should be very small. In mountainous areas however, they can attain values of several hundred milligals. A similar effect can be observed with deflections of the vertical calculated solely from topographic masses in mountainous areas. These values will be much larger than their true values, again suggesting a compensation beneath the mountains.

Thus, not only the visible topography but the gravitational effect of its isostatic compensation must be computed according to some theory of isostacy. Traditionally, the theory of Airy-Heiskanen has been used and this theory was also used in this study.

According to this theory, the mountains, with constant density ρ_o are theorized to "float" on a denser layer of density ρ_i . As the mountains are in floating equillibrium, the higher the mountains, the deeper are the "roots". Analogously, there are "anti-roots" under the oceans. The thickness of the root, t, is given by;

$$t\Delta\rho = H\rho_o \qquad (15)$$

where H is the height of the topography above sea-level and

$\Delta\rho$ is the density contrast between the crust and the mantle.

Using accepted mean continental values of $\rho_0 = 2.67$ g/cm^3 and

$\Delta\rho = -0.4$ g/cm^3, this becomes;

$$t = \rho_0/\Delta\rho \times H = \frac{6.67}{-0.4} \times H \qquad (16)$$

In this study, we assume a crustal thickness of 32 km for the area, which is again consistent with the best known continental values.

The terrain heights used are located at the nodes of regular square grids, as explained earlier. It is natural then to compute the attraction due to the topographic masses and isostatic compensation from regular rectangular prisms. The width and length of each prism is simply the grid spacing of the particular dtm used. For the topographic effect, the height of the prism is the height above sea-level. For the isostatic effect, the height is the thickness of the "root", and the density contrast between the crust and mantle is used to compute the attraction.

To ensure that T_{II} is a harmonic function, T_{II} must be the potential of a given fixed volume of mass. Thus, the same volume of terrain data should be used for each computation. This computation ideally should extend to such a distance from the computation point that the terrain effects of the distant topography remain constant for the local area of interest.

As an alternative to this procedure, one could use a "residual terrain model", or the residual between a mean elevation surface and the actual topography. This would lead to significant computational savings, as shown by (Forsberg & Tscherning, 1981a). In this case, no isostatic compensation needs to be calculated and, in addition, the computation can be carried out to a fixed distance from each computation point.

Figure 2 shows a representative square prism of topographic or isostatic mass. Let this prism have constant density ρ and be attracting a point mass located at the origin. Then the vertical component of the attraction of the prism on the point mass is given by: (Kellog, 1953)

$$g_z = \frac{-\partial T}{\partial z} = -G\rho \int_{x_1}^{x_2}\int_{y_1}^{y_2}\int_{z_1}^{z_2} \frac{z}{r^3}\, dx\, dy\, dz \qquad (17)$$

where:

G = the universal gravitational constant,
r = distance to the attracted point,

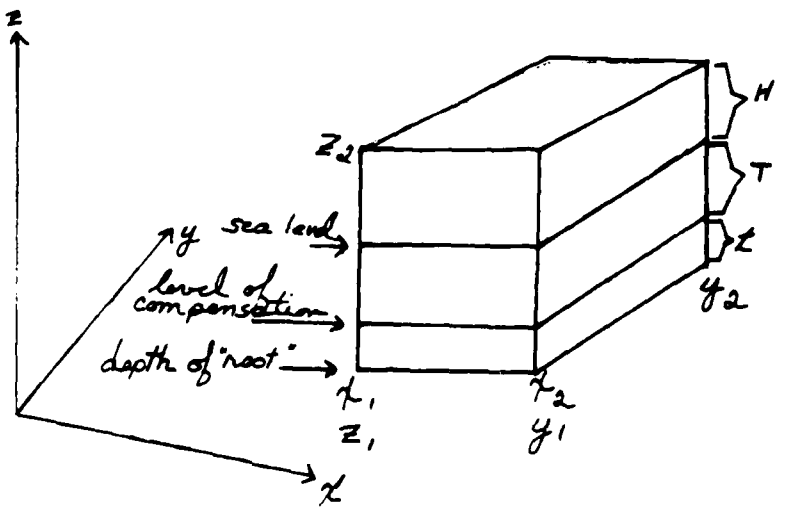

Figure 2. Topographic mass prism.

x,y,z = coordinates of the differential element,
ρ = density of the prism, and,
T = potential of the prism.

Integration of this formula gives; (Forsberg & Tscherning, 1981)

$$g_z = G\rho\left[\left[\left[x\log\left(\frac{y+r_{z_2}}{y+r_{z_1}}\right) + y\log\left(\frac{x+r_{z_2}}{x+r_{z_1}}\right)\right]_{x_1}^{x_2}\right]_{y_1}^{y_2} - z\arctan\left(\frac{xy}{zr}\right)\Bigg|_{x_1,y_1,z_1}^{x_2,y_2,z_2}\right] \quad (18)$$

For prisms which are further away from the attracted point, we may approximate the prism by a horizontal mass plane passing through the center of the prism and parallel to the top and bottom of the prism. In this case, the

attraction in the vertical direction is given by;

$$g_e = -G\rho' \int_{x_1}^{x_2} \int_{y_1}^{y_2} \frac{z_m}{r^3}\, dx\, dy \tag{19}$$

$$= -G\rho' z_m \left(\arctan\left(\frac{xy}{z_m r} \right) \Bigg|_{x_1}^{x_2} \Bigg|_{y_1}^{y_2} \right) \tag{20}$$

where;

$$\rho' = \rho(z_1 - z_2)$$

$$z_m = (z_1 + z_2)/2$$

$$r = (x^2 + y^2 + z^2)^{1/2}$$

To obtain the components of the attraction in the horizontal directions, the coordinate axes of figure 2 are rotated about the origin. Thus, we use the same formulas but with the transformations;

$$(x_1, x_2, y_1, y_2, z_1, z_2)^t = (z_1, z_2, x_1, x_2, y_1, y_2)^t \tag{21}$$

for the north-south component, and,

$$(x_1, x_2, y_1, y_2, z_1, z_2)^t = (y_1, y_2, z_1, z_2, x_1, x_2)^t \tag{22}$$

for the east-west component.

Then the attractions are given by;

$$g_{x,y} = \xi, \eta = \frac{1}{\gamma} g z_{x,y} \tag{23}$$

where g_z has been evaluated according to equation (21) or (22).

For the condensed formulas, integration of equation (19) gives:

$$\xi = g_y = \frac{G\rho'}{\gamma}\left(\log\left(\frac{x + r_{y_2}}{x + r_{y_1}}\right)\Bigg|_{x_1}^{x_2}\right) \tag{24}$$

$$\eta = g_x = \frac{G\rho'}{\gamma}\left(\log\left(\frac{y + r_{x_2}}{y + r_{x_1}}\right)\Bigg|_{y_1}^{y_2}\right) \tag{25}$$

The topographic or isostatic effect on the geoid undulation is obtained by integration of equation (18) with

respect to z;

$$N = G\rho\left(\left[xy\log\left(\frac{z + r_{z_2}}{z + r_{z_1}}\right) + xz\log\left(\frac{y + r_{z_2}}{y + r_{z_1}}\right) + yz\log\left(\frac{x + z r_{y_2}}{x + z r_{y_1}}\right)\right]\Bigg|_{x_1}^{x_2}\Bigg|_{y_1}^{y_2} - \left[\frac{x^2}{2}\arctan\left(\frac{xz}{xr}\right) - \frac{y^2}{2}\arctan\left(\frac{xz}{yr}\right) - \frac{z^2}{2}\arctan\left(\frac{xy}{zr}\right)\right]\Bigg|_{x_1 y_1 z_1}^{x_2 y_2 z_2}\right) \quad (26)$$

For distant prisms, (MacMillan, 1958) has developed simpler expressions for the potential and its derivatives by a spherical harmonic expansion of the prism field. The resulting harmonics are simple polynomials in x, y, and z. The formula for the potential in a coordinate system with origin at the center of the prism and axes perpendicular to the faces is;

$$T = G\rho\Delta x\Delta y\Delta z\left\{\frac{1}{r} + \frac{1}{24r^5}\left[\left(2\Delta x^2 - \Delta y^2 - \Delta z^2\right)x^2 + \left(-\Delta x^2 + 2\Delta y^2 - \Delta z^2\right)y^2 + \left(-\Delta x^2 - \Delta y^2 + 2\Delta z^2\right)z^2\right] + \frac{1}{288r^9}\left[\alpha_1 x^4 + \alpha_2 y^4 + \cdots\right] + \cdots\right\} \quad (27)$$

where, Δx, Δy, and Δz are the sidelengths of the prism.

An even simpler approximation can be made for very distant points. These can be represented as point masses, in which case the potential is given by the first term of equation (27).

It is only through the use of these approximate formulas that the computation of gravimetric quantities from digital terrain models becomes practical. Some preliminary computations were done using only the exact formulas with three digital terrain models having increasingly wider spacing away from the computation point. These were the one degree and five minute matrices described earlier and an additional three second mean elevation matrix. A total of 46,494 prisms must be evaluated for both the topographic and isostatic components when using the one degree mean elevation matrix, the five minute mean elevation matrix and a ten minute by ten minute region of three second mean elvations. This computation took approximately one hour per point on the VAX 11/780 computer system, including cpu time and I/O time. The same computation took approximately 6 minutes per point when a combination of exact and approximate formulas were used. The exact prism formulas were used out to a distance of $\sqrt{6}$ d from the computation point, where d is the length of the main diagonal of the prism being used. The MacMillan formulas were then used out to a distance of $\sqrt{50}$ d from the computation point. At distances further than this, the point mass formula was used. These cut-off distances

have been determined by (Forsberg, 1984) to give a good trade-off between time and accuracy and were verified during this experiment. An exception to this is that the mass plane formulas were always used for geoid undulations.

The topographic and isostatic effects were first calculated for a subset of the observations using a variety of elevation data and techniques to get a feel for the trade-offs in time and accuracy involved. In addition to the 23 points where deflections were known, 52 points where gravity has been observed were used as test points. The one degree mean, five minute mean, and five second point elevation matrices were used alone and in combination with each other. The topographic/isostatic components were then subtracted from the free-air anomalies and known deflections. The results will essentially be the "isostatic anomalies" (Heiskanen & Moritz, 1967) in the case of anomalies and "topographic isostatic deflections" (Heiskanen & Meinesz) in the case of deflections. The results are presented in table 3. The resulting anomalies and deflections should theoretically be small and have low variances. Table 3 can then be used to judge the comparative effectiveness of using various terrain data sets by comparing the means and standard deviations in this table.

Several interesting observations can be made from this table. The inclusion of the five second data marginally improved the results in this case. More important than this

Terrain Data Used	A	B	C	D	E	F
Value						
Δg						
					(1)	(1)
mean	5.73	-5.53	5.33	0.20	-5.56	-0.85
high	24.22	-1.35	24.13	4.44	-0.58	4.09
low	-7.43	-12.61	-5.66	-6.89	-12.25	-7.62
σ	7.80	3.03	6.65	3.04	2.97	2.98
ξ					(2)	(2)
mean	-0.14	-1.87	-1.80	-1.79	-1.57	-1.63
high	3.79	0.53	0.18	0.68	0.40	0.49
low	-4.71	-4.56	-5.00	-4.46	-3.20	-4.76
σ	2.05	1.20	1.18	1.20	1.01	1.20
η					(2)	(2)
mean	-3.83	-0.07	0.11	-0.11	-0.11	-1.62
high	3.09	4.33	4.97	4.34	4.33	2.20
low	-11.56	-6.52	-7.16	-6.55	-6.52	-6.22
σ	5.10	2.49	3.73	3.48	3.51	2.68

Table 3. Observed-component from topographic/isostatic data.

Notes:

(1) Based on n = 40, as 12 points fell outside the innermost terrain data grid.

(2) Based on n = 22, as 1 point fell outside the innermost terrain data grid.

Terrain data grids used:

A - One degree mean elevation grid only.
B - Five minute mean elevation grid only.
C - Five minute mean elevation grid and no bicubic spline interpolation.
D - One degree and five minute elevation grids.
E - Five minute mean and five second mean elvation grids.
F - One degree, five minute and five second grids.

inner grid was the ability to construct a very dense "inner-inner" grid by interpolation of the given elevations in a three by three grid spacing region of the data point. This was accomplished by a bicubic spline interpolation of these elevations. This interpolation was used for all cases except for one case in which only the five minute mean elevations were used. The improvement can be seen by comparing the results obtained from elevation data sets B and C. Note that the results are improved for gravity anomalies but not for deflections, perhaps reflecting that deflections are less affected by the very local topography. Another interesting observation is that, again for anomalies, the use of the one degree mean elevations helps to bring the mean residual very near to zero. This perhaps indicates the desirability of using such a broad and coarsely spaced grid for the outer zones to remove local biases incurred from the inner zone data.

For these cases, the most desirable combinations of elevation data appear to be the one degree mean grid with the five minute mean grid, using an interpolation to densify the five minute grid in the vicinity of the computation point and this same data set with also the five second elevation data, or data sets D and E, according to table 2.

To provide a wide variety of cases for the least squares collocation program, another larger set of observations were used as test points. Using the one degree and

at 500 points within the test region. Using this elevation data together with the five second point elevation grid, anomalies were computed for a subset of 110 of these points. Both sets of test points were chosen to be well distributed spatially and to have the same elevation histogram as the original 1062 points. The average spacing between the points was about 1 arc minute. In addition, the undulation was computed at the six coarser points using the second elevation data set. The locations of the test points are shown in figure 3.

The values computed from the terrain data were then subtracted from the free air gravity anomalies and observed undulations. The results are shown in table 4.

Terrain Data Used	D	F
n	500	110
Mean	-11.62	-14.52
Min	4.43	0.43
Low	-34.35	-36.50
RMS	15.37	17.97
σ	9.57	10.50

Table 4. Gravity anomaly residuals (observed-computed from topographic/isostatic data.

Terrain Data:

D - One degree and five minute mean elevations.
F - One degree, five minute, and five second elvation

For geoid undulations, the one degree and five minute

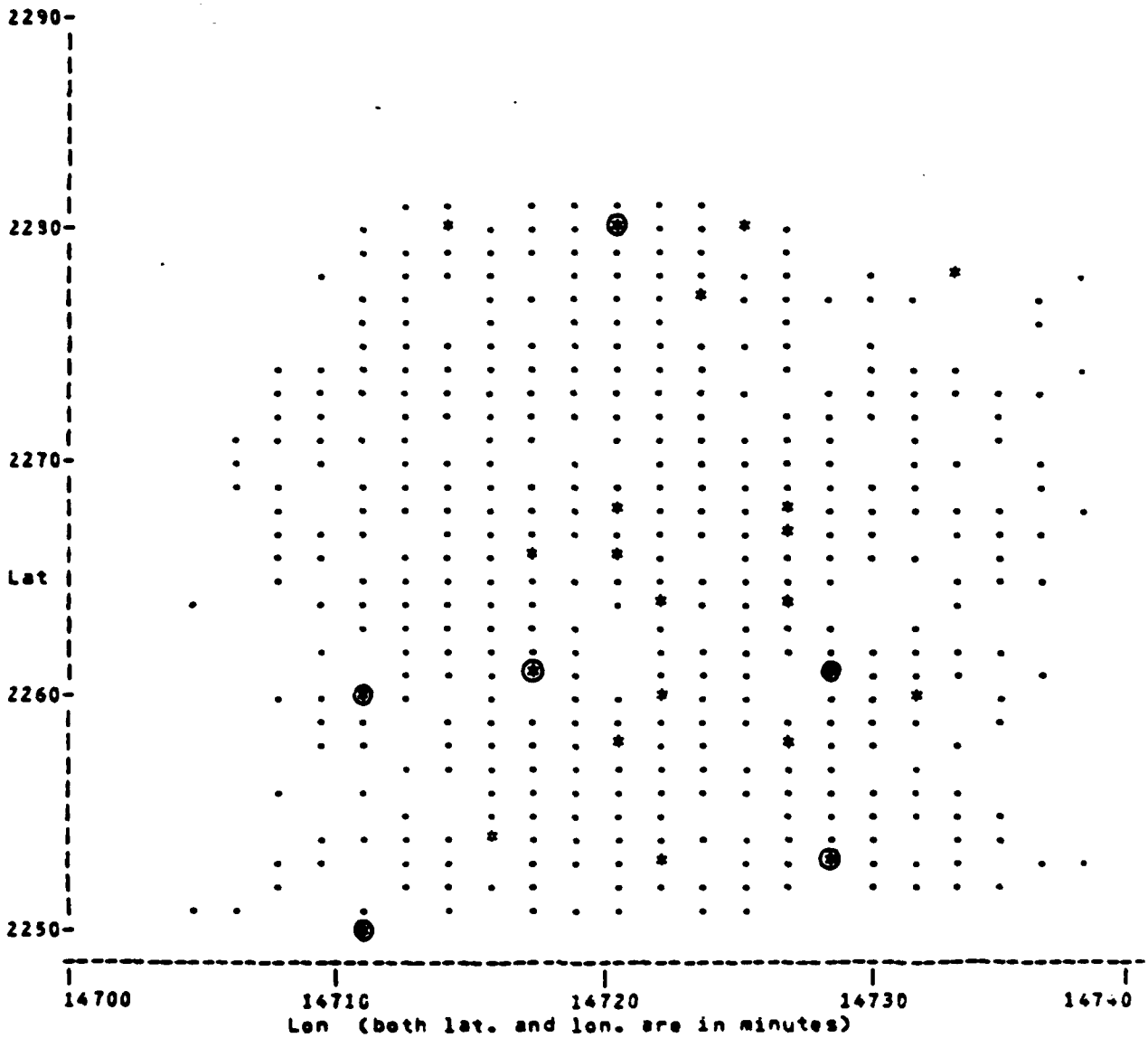

Figure 3. Observation data.

Legend:

. = Gravity Anomaly Observation
* = Deflection Observation
o = Doppler Station

data sets (Terrain Data A of table 3) were used. The results were poor, with a mean error of -3.03 meters and a standard deviation of the error of around 0.3 meters. A possible explanation is the "indirect effect" of the topographic/isostatic reduction. Heiskanen and Moritz (1967) state that this effect can be on the order of 10 meters. It would be a relatively simple matter to check on this by computing the potential due to the topography seperately from that computed from the isostatic compensation. Dividing the difference between the two by normal gravity will give the indirect effect on geoid undulation. This was not done in this study.

COMPUTATION OF THE RESIDUAL COMPONENT

The residual component, the component not modeled by either the global earth model or the topography-isostacy was computed by least squares collocation. The topographic-isostatic components of gravity anomalies, deflections, and undulations were added to the corresponding global earth model components. These sums were then subtracted from the observed data to give "residual" observations. These were used to compute residual values at other known points which were not used as observations. The predicted residuals were then compared with the known residuals. The statistics of the residual observations are given in table 5.

Terrain Data		D	=
Value			
Δg	n	500	110
	mean	-4.74	-7.36
	high	14.85	9.10
	low	-26.07	-27.63
	σ^2	92.90	83.71
	n	23	23
	mean	3.31	3.47
ξ	high	5.86	5.89
	low	0.87	0.57
	σ^2	1.53	1.76
	n	23	23
	mean	0.92	-0.61
η	high	5.23	3.14
	low	-5.57	-5.28
	σ^2	11.74	7.03
N	n	5	
	mean	-8.03	(not computed)
	high	-7.18	
	low	-9.42	
	σ^2	0.60	

Table 5. Residual values (observed-(TI & EM)).

The goal of reducing the observations before applying collocation was to smooth out the gravity field, or reduce the range of values and the variance of the gravity anomalies. From table 5, we see that the variance of the anomalies has been reduced from 470.96 to between 30 and 90 depending on the elevation data used. Comparison with table 1 shows that the variance of all of the quantities has been reduced. Another desirable attribute of a "smooth" gravity field is that the mean values of the quantities g, ξ, η, and N be near to zero. The mean of the unreduced anomalies was -14.60 mgals while that of the reduced values is -4.74 mgal for the best case. The means of the deflection components are also brought nearer to zero by the reduction and so is that of the undulations.

These residual observations were then used to form the observation equations for least squares collocation. The basic form of an observation equation without parameters is, (Moritz, 1972):

$$x = s + n \qquad (23)$$

where:

x = a vector of observations, in this case, residual gravity anomalies, deflections, and geoid undulations,

s = the unknown "signal" portion of the

observation, and,

n = a random "noise" component.

The quantities s and n are assumed to be uncorrelated, zero-mean quantities with Gaussian distributions. To predict the signal, $\tilde{s}$, at other unknown points, the least squares collocation formula for the minimum variance estimate is:

$$\tilde{s} = C_s^t \bar{C}^{-1} x \qquad (29)$$

where;

C_s = cov(s,s), the matrix of covariances between the quantity being estimated and the observations, and

$\bar{C}$ = (cov(s,s) + cov(n,n)), the sum of the matrix of covariances among and between the observations and the covariance matrix of the noise vector.

Since the quantities we wish to estimate are linear functionals of the anomalous potential T, it suffices to determine an expression for the spatial covariance of T and then to apply the law of propagation of covariances (Moritz, 1972) to this expression to obtain the covariances between all of the observations and predictions. Let K(P,Q) be the covariance between T at point P and T at point Q. Now let a

and b be the two quantities derived from f by linear operations such as differentiation or multiplication by a constant. If we wish to symbolize these operations by A(T) and B(T), then the covariance between a_P and b_Q is given by:

$$C(a_P, b_Q) = \mathrm{cov}(a_P, o_Q) = A(B(K(P,Q))) \qquad (30)$$

The least squares collocation program of (Tscherning, 1974) was used. This program allows the specification of one of three isotropic (azimuth independent) covariance functions which are all based on one of the anomaly degree models developed by (Tscherning & Rapp, 1974). The "degree variances" of the gravity anomalies are given by (Heiskanen and Moritz, 1967):

$$c_n = \sum_{m=0}^{n} (\bar{a}_{nm}^2 + \bar{b}_{nm}^2) \qquad (31)$$

where:

a_{nm}, b_{nm} = fully normalized spherical harmonic coefficients of the gravity anomalies.

We can then write an expression for the covariance

function of the gravity anomalies as;

$$C(P,Q) = \mathrm{cov}(\Delta g_P, \Delta g_Q) = \sum_{n=0}^{\infty} C_n P_n(\cos\psi)\left(\frac{R^2}{rr'}\right)^{n+2} \qquad (32)$$

where;

P = the legendre polynomial of degree n,
ψ = the spherical distance between P and Q,
R = radius of the Bjarhammer sphere,
r = distance from P to the origin, and,
r' = distance from Q to the origin.

The degree variances of the anomalous potential are related to those of the gravity anomalies by;

$$k_n = \frac{R^2}{(n-1)^2} C_n \qquad (33)$$

where;

R = the mean earth radius.

We can write an expression for the covariance of the anomalous potential as;

$$K(P,Q) = K(\psi) = \sum_{n=0}^{\infty} K_n P_n(\cos\psi) \qquad (34)$$

The model used for the anomaly degree variances was;

$$c_i = \frac{A\,(1-1)}{(1-2)(1+B)} \qquad (35)$$

where the constants A and B are determined from the variance of the observed gravity anomalies.

The method of collocation also gives an estimate of the mean square error of prediction as:

$$m_s^2 = C_{ss} - C_s^t \bar{C}^{-1} C_s \qquad (36)$$

where: $C_{ss} = \mathrm{cov}(s_p, s_p)$, the point variance of the quantity estimated.

In this case, however, we know exactly the error of the estimate since we are predicting at known points.

Several cases, involving different subsets of observations and predictions, were run. The observation points were selected to have an average spacing of approximately 5 arc minutes. The data used in the various cases of collocation are identified in table 6.

Cases	Data
I	Unreduced.
II	Reduced with topographic data set C and Rapp 180.
III	Reduced with Topographic data set F and Rapp 180.
IV,V	Same as III
VI	Reduced only with topographic data set F.

Table 6. Identification of collocation cases.

The results of collocation are shown in table 7. We can see that the results for gravity anomalies are significantly improved by using the observations reduced with some topographic data. The use of the spherical harmonic coefficients does not affect the results for gravity anomalies. The best level of accuracy obtained in this test was 3 milligals (one sigma). This result was obtained by using 300 gravity anomaly observations, spaced about 5 minutes apart. The inclusion of deflection or undulation observations does not appear to affect the results for gravity anomalies. Meanwhile, by increasing the number of anomaly observations by a factor of 3, we gain about one milligal in accuracy.

For deflections, the best accuracies, again in terms of standard deviation of the errors, for ξ and η are 0.79 arc seconds and 0.99 arc seconds

Case	observations		(observation - predicted) n	max	mean	std. dev.
I	Δg	100	400	20.25	-1.21	6.80
	ξ	3	20	2.69	-0.62	1.11
	η	3	20	-3.13	-0.61	1.22
	N	0	6	-27.35	-25.00	0.50
II	Δg	100	400	-16.37	-0.14	4.15
	ξ	3	20	-3.96	-0.12	1.34
	η	3	20	5.21	3.25	1.54
	N	0	6	-3.25	-3.00	0.50
III	Δg	100	400	-16.37	-0.14	4.15
	ξ	3	20	-3.44	0.12	1.36
	η	3	20	2.68	0.65	1.13
IV	Δg	300	200	-12.52	0.26	3.00
	ξ	3	20	-3.81	0.16	1.39
	η	3	20	1.97	0.12	0.97
V	Δg	300	0			
	ξ	5	18	2.67	1.18	0.92
	η	5	18	-2.01	-0.08	0.94
VI	Δg	300	200	-12.61	0.23	3.03
	ξ	3	20	-4.91	-1.61	0.79
	η	3	20	-1.49	0.09	0.89

Table 7. Collocation results..

graphic and isostatic reductions, neglecting the Rapp 180 components. The maximum and mean errors for the north-south component are slightly greater however, than when the Rapp 180 coefficients are used. The benefit of using the five second inner grid data is likewise to bring the mean errors closer to zero, the standard deviation remaining the same.

The case of undulations is even harder to analyze, given only six observations. From this test, we would conclude that the best way to estimate these is strictly from the spherical harmonic coefficients. The effects of reducing the observations and applying collocation degraded the results obtained only with the spherical harmonics.

CONCLUSIONS AND RECOMMENDATIONS

A technique for computing a local gravity field model in mountainous terrain has been tested. The results indicate that gravity anomalies can be predicted with an accuracy of 3 milligals, deflections of the vertical with an accuracy of about 1 arc second and geoid undulations with an accuracy of about 1.0 meters.

For gravity anomalies, least squares collocation following trend removal by topographic/isostatic data and spherical harmonic coefficients gave the best results. For deflections, the inclusion of the spherical harmonic component helped reduce a bias in the errors. For undulations, the best results were obtained directly from the spherical harmonic coefficients, neglecting any topographic data or least squares collocation.

The best combination of terrain data appears to be a widely spaced (about 1 degree) outer grid extending to at least 10 degrees around the test points and at least one coarser inner grid (about 5 minutes) extending to about 5 degrees from the computation point. The results are significantly enhanced by interpolating this inner grid to an even finer grid in the very near vicinity of the computation point. When this type of interpolation is done, it may be unnecessary to include a very fine grid of elevations as a third "inner-inner" zone.

There exist very efficient computer programs for performing all of the calculations described herein. Given a medium sized minicomputer, all of the calculations can be carried out in a few hours. The topographic/isostatic computation is the most time-consuming but, using approximate formulas, these can be done in a reasonable time.

For adjusting triangulation networks, or reducing horizontal and vertical angles to the ellipsoid, the accuracy of the vertical deflections obtained herein is sufficient for even first order work. If the elevation is 7 degrees, an error in deflection of the vertical of 2 arc seconds will result in an error of 0.25 seconds in horizontal angles, which is below the observation error of most angles.

In mountainous areas, conversion of satellite-derived heights to heights above sea level requires the geoid undulation. This study indicates that these can be computed to an accuracy of about 1 meter, which is consistent with past results. This will propogate directly into a 1 meter error in sea-level heights, naturally. In the absence of other information, this may be an acceptable error for some work.

The accuracy of the gravity anomalies, 3 milligals, means that they could be used ,for instance, to compute deflections of the vertical and geoid undulations through Vening Meinesz' and Stokes' integrals respectively. The predicted anomalies could also be useful in geophysical

explorations.

For alignment and correction of inertial navigation systems, the accuracies obtained for deflections and anomalies could be useful in certain applications. This area must be explored further however.

REFERENCES

Carlson, A., Collocation Prediction Techniques: Test and Evaluation, Defense Mapping Agency, Hydrographic/Topographic Center, (unpublished), Washington, D. C., April, 1983.

Defense Mapping Agency, Department of Defense World Geodetic System 1972, Technical Report 0002, January, 1974.

Forsberg, R., A Study of Terrain Reductions, Density Anomalies and Geophysical Inversion Methods in Gravity Field Modelling, The Ohio State University, Department of Geodetic Science and Surveying, report number 335, Columbus, Ohio, April, 1984.

Forsberg, R., and Madsen, F., Gravity Prediction in Northern Greenland Using Collocation and Digital Terrain Models, paper presented at the symposium, "Space Geodesy and Its Applications", Cannes, France, 1980.

Forsberg, R., and Tscherning, C., "The Use of Height Data in Gravity Field Approximation by Collocation", Journal of Geophysical Research, volume 86, number B9, pp. 7834 - 7854, September, 1981a.

Forsberg, R., and Tscherning, C., Gravity Determination in the Norwegian-Greenland Sea. An Assessment of Recent Results, paper presented at Fourth Discussion Meeting on the Blue Road Geotraverse, Berlin Free University, February, 1981b.

Gurtner, W. and Elmiger, A., Computation of Geoidal Heights and Vertical Deflections in Switzerland, Proceedings of the International Association of Geodesy (IAG) Symposia, International Union of Geodesy and Geophysics (IUGG), XVIII General Assembly, Hamburg, FRG, August, 1983.

Heiskanen, W. and Meinesz, V., The Earth and Its Gravity Field, McGraw-Hill Book Company, New York, New York, 195

Heiskanen, W., and Moritz, H., Physical Geodesy, W. H. Freeman and Company, San Francisco, California and London, U. K., 1967.

Kellog, O., Foundations of Potential Theory, Dover Publications, Inc., New York, New York, 1953.

Lachapelle, G., Determination of the Geoid Using Heterogeneous Data, Ph. D. dissertation, Institute of Physical Geodesy, The Technical University of Graz, Graz, Austria, 1975.

MacMillan, W., Theoretical Mechanics, vol. 2: The Theory of the Potential, Dover Publications, Inc., New York, New York, 1958. (cited in Forsberg and Tscherning, 1981a)

Moritz, H., Advanced Least Squares Methods, The Ohio State University, Department of Geodetic Science and Surveying, report number 175, Columbus, Ohio, June, 1972.

Rapp, R., A Global 1 deg. X 1 deg. Anomaly Field Combining Satellite, Geos-3 Altimeter and Terrestrial Data, The Ohio State University, Department of Geodetic Science and Surveying, report number 276, Columbus, Ohio, 1978.

Rapp, R., The Earth's Gravity Field to Degree and Order 180 Using Seasat Altimeter Data, Terrestrial Data and Other Data, The Ohio State University, Department of Geodetic Science and Surveying, report number 322, Columbus, Ohio, December, 1981.

Sunkel, H., The Geoid in Austria, Proceedings of the International Association of Geodesy (IAG), Symposia, International Union of Geodesy and Geophysics (IUGG), XVIII General Assembly, Hamburg, FRG, August, 1983.

Tscherning, C., A Fortran IV Program for the Determination of the Anomalous Potential Using Stochastic Least Squares Collocation, The Ohio State University, Department of Geodetic Science and Surveying, report number 203, Columbus, Ohio, July, 1974.

Tscherning, C. and Rapp, R., Closed Covariance Expressions for Gravity Anomalies, Geoid Undulations, and

Deflections of the Vertical Implied by Anomaly Degree Variance Models, The Ohio State University, Department of Geodetic Science and Surveying, report number 209, Columbus, Ohio, May, 1974.

Todd, M., Rapid Geodetic Survey System (RGSS) Deflection of the Vertical and Gravity Anomaly Tests at White Sands Missile Range, 1980, ETL-0303, U. S. Army Engineer Topographic Laboratories, Fort Belvoir, Virginia, October, 1982.